APPLIED PHYSICS LETTERS **90**, 212501 (2007)

Enhanced current flow through meandering grain boundaries in $YBa_2Cu_3O_{7-\delta}$ films

Rafael B. Dinner, Kathryn A. Moler,[a] and M. R. Beasley
Geballe Laboratory for Advanced Materials, Stanford University, Stanford, California 94305

D. Matthew Feldmann
Los Alamos National Laboratory, Los Alamos, New Mexico 87545

(Received 24 January 2007; accepted 25 April 2007; published online 21 May 2007)

In $YBa_2Cu_3O_{7-\delta}$ (YBCO) coated conductors grown by metal organic deposition, in-plane meandering of grain boundaries (GBs) has been linked to higher critical current density. The authors investigate this link in individual GBs using transport measurements and scanning Hall probe microscopy with current reconstruction. They observe current-induced flux entry into a coated conductor, then model its behavior by imaging YBCO films with single, straight GBs tilted at various angles to the applied current. They find a strong dependence of critical current on angle, sufficient to explain the enhancement observed for meandering GBs. © *2007 American Institute of Physics*. [DOI: 10.1063/1.2740610]

High-temperature superconductors are being engineered for use in high-current applications, including motors, generators, and power lines.[1] In the coated conductor architecture, a $YBa_2Cu_3O_{7-\delta}$ (YBCO) film is grown on a flexible metal tape. The tape is polycrystalline, and its crystal grains give rise to separate grains in the superconducting layer. Grain boundaries (GBs) admit magnetic flux at lower-current densities J_b than the intragranular YBCO's critical current density J_c; J_b decreases exponentially with GB angle.[2] Much progress has been made by improving substrates to align the grains to within a few degrees[3,4] and elongate the grains in the direction of current flow.[5] In the superconducting layer, GBs can be further engineered. For example, chemical doping improves J_b under some conditions.[6] In this work, we examine a geometric effect arising from the YBCO growth method.

A recent study[7] compared YBCO coated conductors grown on rolling assisted biaxially textured substrates (RABiTS) by pulsed laser deposition (PLD) and metal organic deposition (MOD). While the films had similar *intragrain* critical current densities J_c, the MOD film had four times higher *intergrain* critical current density J_b. The two growth methods could produce GBs with different chemical or atomic-scale effects, but the study suggested that the different J_b values stem from the micron-scale geometry of the GBs: The PLD films replicate the straight GBs of the substrate, while MOD GBs meander relative to these straight boundaries. A meandering GB crossing a given link will be longer than its straight counterpart. Thus, meandering will increase J_b, calculated by dividing the link's critical current I_c by its cross-sectional area, even for a constant $J_{b\perp}$, the current density locally perpendicular to each point of the GB, calculated by dividing I_c by the GB's area.

Here, we use magnetic imaging and transport measurements to confirm that the meandering geometry of MOD films' GBs is sufficient to explain their enhanced J_b. Our images show that down to the instrumental resolution of 1 μm, supercurrents redirect to take advantage of GB meandering, achieving a higher macroscopic J_b for the same microscopic $J_{b\perp}$.

The magnetic images are obtained with a custom-built large-area scanning Hall probe microscope.[8] As a 400 Hz sinusoidal current is applied to the sample, a Hall sensor rasters over the sample surface, pausing at each pixel location to measure $B_z(t)$ over the full cycle of applied current. The data are later assembled into a series of images, each corresponding to a particular phase—and applied current—within the cycle.

We first image a MOD film—a 400 nm thick YBCO coated conductor grown by American Superconductor on RABiTS. Figure 1(a) shows the sample geometry, defined by laser cuts through the film. The cuts direct the applied current to flow through a 200 μm wide × 450 μm long link. The link is held at 40 K and carries 1.3 A (well below I_c) at the peak of the ac cycle. As depicted by the pink arrows within the scan area in Fig. 1(a), the current flows along the link at the bottom edge of the laser cut, and shielding current flows around the isolated section of YBCO that constitutes its upper edge, in response to the field generated by the link.

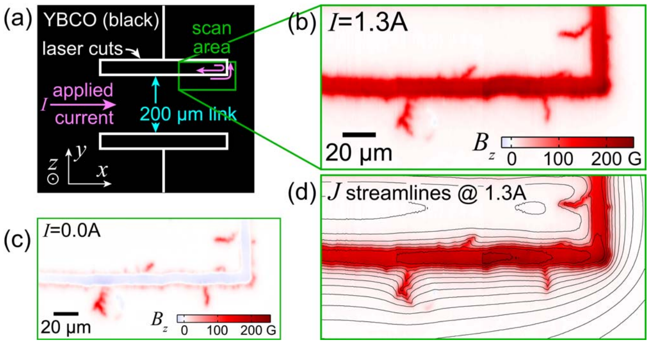

FIG. 1. (Color online) (a) Sketch of a MOD coated conductor, in which laser cuts through the film define a bridge that channels the applied current. (b) Magnetic field B_z over a section of the bridge, imaged via scanning Hall probe microscopy. Current forces flux into the film's meandering grain boundaries. (c) Flux remains trapped when the current returns to zero. (d) Reconstructed current streamlines overlaid on B_z show that the current spreads out along the boundaries, and its direction varies to accommodate their meandering. 40 mA flows between neighboring streamlines.

---

[a] Electronic mail: kmoler@stanford.edu

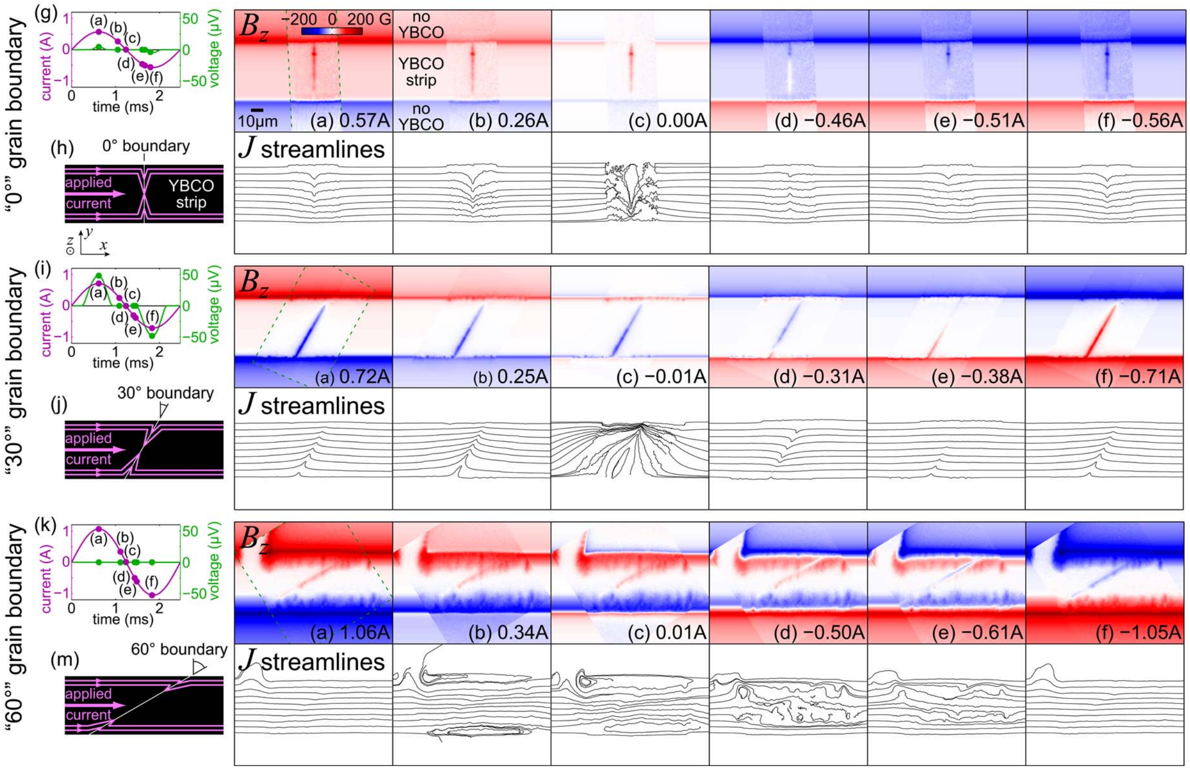

FIG. 2. [(a)–(f)] Magnetic images B_z and reconstructed streamlines of current J for each of three samples with grain boundaries tilted, as shown in (h), (j), and (m). The boundary between data and background calculation is identified in the (a) frames by a dashed green box. The magnetic images are all on the same color scale, shown in (a). See Ref. 9 for the full set of images presented as a movie. (g), (i), and (k) each plot one cycle with the applied currents and measured voltages for frames (a)–(f).

These currents force flux into the film from the edges, primarily along the narrow, cracklike features seen in the magnetic image, Fig. 1(b). As the applied current returns to zero in Fig. 1(c), flux remains trapped; thus these features are not actual cracks but instead support supercurrent, albeit with a lower J_c than the surrounding material. The complete time evolution over a cycle of applied current is presented as a movie in the supplemental material.[9] Combined magneto-optic and grain mapping studies of similar samples have shown that such features are GBs.[10] Our image reveals that the GBs are not straight. By reconstructing the current density **J** from the magnetic image,[11,12] we show in Fig. 1(d) that **J** does change direction to accommodate the shape of the meandering GBs, at least down to the length scales of the instrument resolution of about 1 μm.

To model the behavior of a local segment of a meandering GB, we fabricate straight GBs tilted at 0°, 30°, and 60° in-plane angles across links of fixed width (50 μm), depicted in Figs. 2(h), 2(j), and 2(m). We also measure a 50 μm $\times$ 500 μm link with no GB. The GB's length increases as it tilts toward the direction of current flow between the grains. We pattern the samples from two nominally identical 180 nm thick YBCO films, grown epitaxially by pulsed laser deposition on $SrTiO_3$ bicrystals, each with a straight, symmetric 5° [001]-tilt GB. The 0° link, Fig. 2(h), and the link with no GB occupy one film, while the 30° and 60° links are patterned at different points along the GB of the second film.

Table I presents current-voltage characteristics of the links in zero field at 77 K with a critical voltage criterion of 50 nV. Instead of a constant $J_{b\perp}$, we find it increases with GB tilt, exceeding the expected geometric effect of lengthening the GB. In fact, at 60° tilt, J_b is equal to the measured intragrain value, as if the GB were completely transparent to the current. This strong dependence of J_b on tilt motivates our more detailed study of these samples via magnetic imaging.

Noise characteristics of the Hall sensor force us to image at 40 K rather than 77 K. We therefore also measure current-

TABLE I. Critical current densities of tilted grain boundaries (GBs). The last row compares the intragrain J_c. The “CR” column compares current density perpendicular to the GBs as reconstructed from magnetic images at 40 K.

	J_b (MA/cm^2)		$J_{b\perp}$ (MA/cm^2)		
Sample	77 K	40 K	77 K	40 K	CR
0° GB	1.4	5.6	1.4	5.6	4.6
30° GB	1.8	4.9	1.6	4.3	3.5
60° GB	4.7	>11.8	2.4	>5.9	4.5
No GB	4.7	12.6			